

COMPARISON OF CLOUD MOTION VECTOR HEIGHT ASSIGNMENT TECHNIQUES USING THE GOES-12 IMAGER

Anthony J. Schreiner¹, W. Paul Menzel², Andy Heidinger², Jim Davies¹, Wayne Feltz¹

¹ - Cooperative Institute for Meteorological Satellite Studies

² - NOAA/NESDIS

1225 West Dayton Street, Madison, Wisconsin 53706, USA

ABSTRACT

Geostationary Operational Environmental Satellite, GOES-12, cloud motion vector heights are assigned by one of two techniques. In opaque clouds, infrared window (IRW at 10.7 μm) brightness temperatures are compared to forecast temperature profiles to infer the level of best agreement that is taken to be the level of the cloud. In semi-transparent clouds or sub-pixel clouds, since the observed radiance contains contributions from below the cloud, this IRW technique assigns the cloud too low a level. Corrections for the semi-transparency of the cloud are accomplished with a simplified version of the carbon dioxide slicing technique; radiances with similar ice cloud emissivities and sensitive to different layers of the atmosphere (CO_2 at 13.3 μm and IRW at 10.7 μm) are combined via a ratio technique to infer the level of the cloud. Prior to GOES-12, the IRW-water vapor (H_2O) intercept technique was used to perform a correction for cloud semi-transparency; radiances sensitive to water vapor (H_2O at 6.5 μm) and radiances not sensitive to water vapor (IRW at 10.7 μm) exhibit a linear relationship as a function of cloud amount that is used to extrapolate the correct height. The cloud heights inferred from CO_2 slicing and IRW-water vapor intercept techniques differ somewhat; this paper offers another height comparison separating water from ice clouds (sorted by coincident Moderate resolution Imaging Spectro-radiometer 8.6 and 11 μm imagery) and uses radiative transfer physics to understand the height differences.

1. TECHNIQUE DESCRIPTIONS

Cloud motion vectors are often inferred from tracking semi-transparent or sub-pixel clouds. Height assignments are difficult because cloud amount and cloud emissivity are less than unity by unknown amounts; low thick clouds cannot easily be separated from high thin clouds. The infrared window (IRW) technique works reliably only in opaque clouds; IRW brightness temperatures can be compared to forecast temperature profiles to infer the level of best agreement that is taken to be the level of the cloud. In semi-transparent ice-clouds, the carbon dioxide (CO_2) slicing technique (Menzel et al., 1983) combines radiances that have similar ice cloud emissivities and that are sensitive to different layers of the atmosphere (CO_2 at 13.3 μm and IRW at 10.7 μm) via a ratio technique to infer the level of the cloud. In semi-transparent water clouds or sub-pixel clouds, a similar concept is used in the water vapor intercept technique (Szejwach, 1982), where the fact that radiances influenced by upper tropospheric moisture (H_2O at 6.5 μm) and radiances not sensitive to water vapor (IRW at 10.7 μm) exhibit a linear relationship as a function of cloud amount is used to extrapolate the correct height.

The CO_2 slicing technique cloud height uses a ratio of deviations in observed cloudy radiances from corresponding clear air radiances for IRW and CO_2 channels. The clear and cloudy radiance differences are determined from observations with GOES-12 and radiative transfer calculations. The cloud emissivities of

the two channels are roughly the same for ice clouds so the ratio of the clear and cloudy radiance differences yields a solution for the cloud top pressure of the cloud within the field of view (FOV). The observed differences are compared to a series of radiative transfer calculations with different cloud pressures; the cloud top pressure belongs to the calculation that best satisfies the observations (Menzel et al. 1983, Merrill et al. 1991).

The H₂O intercept height assignment is predicated on the fact that the radiances for two spectral bands vary linearly with cloud amount. Thus a plot of H₂O (6.5 μm) radiances versus IRW (10.7 μm) radiances in a field of varying cloud amount will be nearly linear. These data are used in conjunction with forward calculations of radiance for both spectral channels for opaque clouds at different levels in a given atmosphere specified by a numerical weather prediction of temperature and humidity. The intersection of measured and calculated radiances will occur at clear sky radiances and cloud radiances. The cloud top temperature is extracted from the cloud radiance intersection (Schmetz et al., 1993). This technique provides heights for mid- to upper tropospheric clouds.

Water and ice clouds have been sorted using an IR-based MODIS cloud thermodynamic phase product; using 8.5 and 11 μm measurements (Baum et al. 2000). The IR phase retrieval provides four categories: *ice*, *water*, *mixed phase*, and *uncertain*. A “mixed phase” cloud is thought to consist of a mixture of ice and water particles. The IR-based cloud phase method relies on the brightness temperature difference (BTD) between the 8.5 and 11 μm brightness temperatures (BTD[8.5-11]) as well as the 11-μm brightness temperature. The imaginary component of the index of refraction differs for ice and water at these two wavelengths. The BTD[8.5-11] is affected by atmospheric water vapor absorption, surface emissivity, and cloud particle size (small particles scatter more radiation than large particles). Radiative transfer simulations show that for ice clouds, BTD[8.5-11] tends to be positive in sign, whereas for low-level water clouds, BTD[8.5-11] tends to be very negative. This simple bi-spectral IR technique is adequate for classifying the phase as either “ice” or “water” for about 80% of the cloudy pixels on a global basis. Problems occur in optically thin cirrus, multilayered clouds (especially thin cirrus over lower-level water clouds), and single-layered clouds having cloud top temperatures from 233K to 273K (i.e., super-cooled water or “mixed phase” clouds).

The multi-spectral imager from GOES-12 measures IRW (centered at 10.7 μm) and H₂O (centered at 6.5 μm) radiances from 4 km FOVs and CO₂ (centered at 13.3 μm) radiances from 8 km FOVs. All three cloud height assignment techniques can be compared with simultaneous measurements from the GOES-12 imager. The clouds can be separated into ice and water cloud classes using collocated MODIS measurements.

2. RADIATIVE TRANSFER CONSIDERATIONS

2.1. Brightness temperature sensitivity to ice clouds

To explore the sensitivity of water vapor (MODIS ch 27 at 6.5 μm), infrared window (MODIS ch 31 at 11 μm), and carbon dioxide (MODIS ch 33 at 13.3 μm) channels to the height of optically thin clouds, a radiative transfer calculation was performed using a standard adding/doubling approach with delta-*M* scaling of the phase function (Wiscombe 1977). A correlated-*k* approach was used to model gaseous absorption by H₂O, CO₂, O₃, CO, CH₄, O₂, NO, and other trace gases (Bennartz and Fischer 2000; Kratz 1995). Both water and ice cloud particles were taken to be spheres at all wavelengths, and Mie scattering was assumed. Figure 1 reveals that the CO₂ channel shows higher sensitivity to the height of high thin clouds (9 K) than the H₂O channel (5 K); sensitivity to low thin clouds is sustained in the CO₂ channel but disappears in the H₂O channel.

2.2. Weighting functions in the presence of ice clouds

To explore from what layers in the cloud and atmosphere the radiation in the water vapor and carbon dioxide channel is emanating from, forward calculations were performed using LBLDISv1.2 (which combines clear sky LBLRTMv6.01 evolved from Clough et al. 1992 and ice cloud DISORTv2.0 derived from Stamnes et al. 1988). The cloud layer from 300 to 375 hPa was constructed from Mie spheres with effective diameter of 100 μm; optical depths (OD) of 0.5 and 2.0 at 10 μm were used. Weighting functions for nadir view for measurements at 13.3 μm (752 1/cm) and 6.7 μm (1492 1/cm) with 0.6 1/cm bandwidth are shown in Figure 2. The 6.7 μm sees deeper into thin ice clouds (OD of 0.5 at 10 μm) than the 13.3 μm; in thicker clouds (OD

of 2.0 at 10 μm) this is no longer so. Note that an effective cloud amount of 0.4 (0.87) is equivalent to an OD of 0.5 (2.0) at 10 μm .

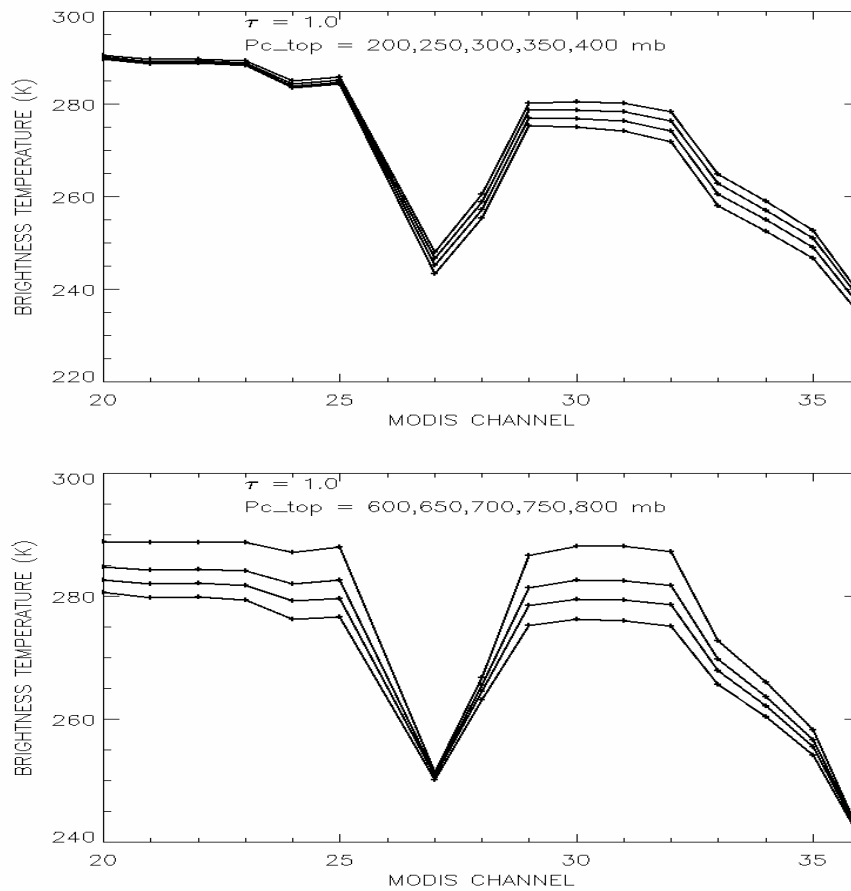


Figure 1: Sensitivity of H₂O (MODIS ch 27 at 6.5 μm), IRW (MODIS ch 31 at 11 μm) and CO₂ (MODIS ch 33 at 13.3 μm) brightness temperatures to cloud height of optically thin clouds (visible optical depth 1) located high (top panel) in the troposphere (at 200 to 400 hPa) and low (bottom panel) in the troposphere (600 to 800 hPa).

3. COMPARISONS AND VALIDATIONS

3.1. Comparison with lidar heights

The GOES-12 cloud top pressures (CTP inferred from CO₂/IRW slicing for semi-transparent ice clouds and IRW technique for opaque clouds) were compared to airborne lidar (Cloud Physics Lidar - CPL) determinations of cloud height for 5 December 2003 from 1700 to 1830 UTC. CTPs were converted to heights using coincident radiosondes near the U.S. Department of Energy (DOE) Cloud and Atmospheric Radiation Testbed. (CART-site). Figure 3 shows that GOES and CPL heights compare within better than 1 km for most of the flight track; notable exceptions occur at 17.3, 17.5 and 18.2 UTC when GOES places the cloud more than 5 km too low (this could be semi-transparent high cloud that is not detected by CO₂ slicing and is assigned to be lower opaque cloud by the IRW technique).

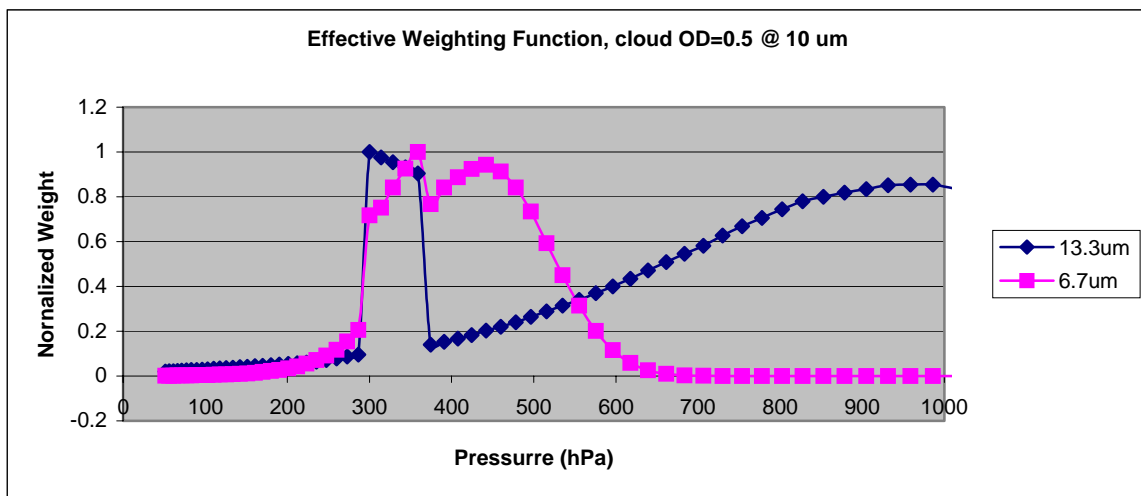
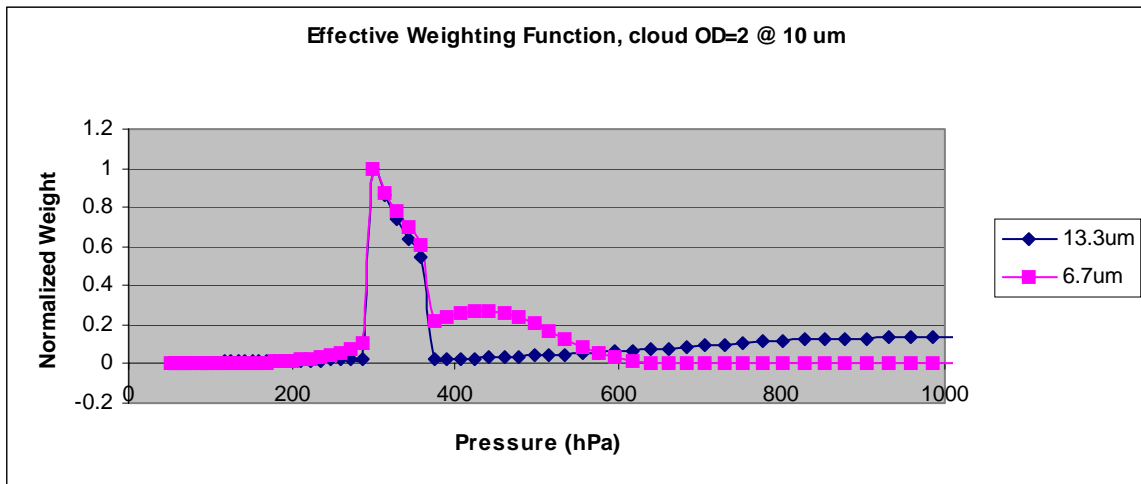


Figure 2: Weighting functions for nadir view for measurements at 13.3 μm (752 1/cm) and 6.7 μm (1492 1/cm) viewing a cloud layer from 300 to 375 hPa composed of Mie spheres with effective diameter of 100 μm and optical depth of 2.0 (top) and 0.5 (bottom) at 10 μm .

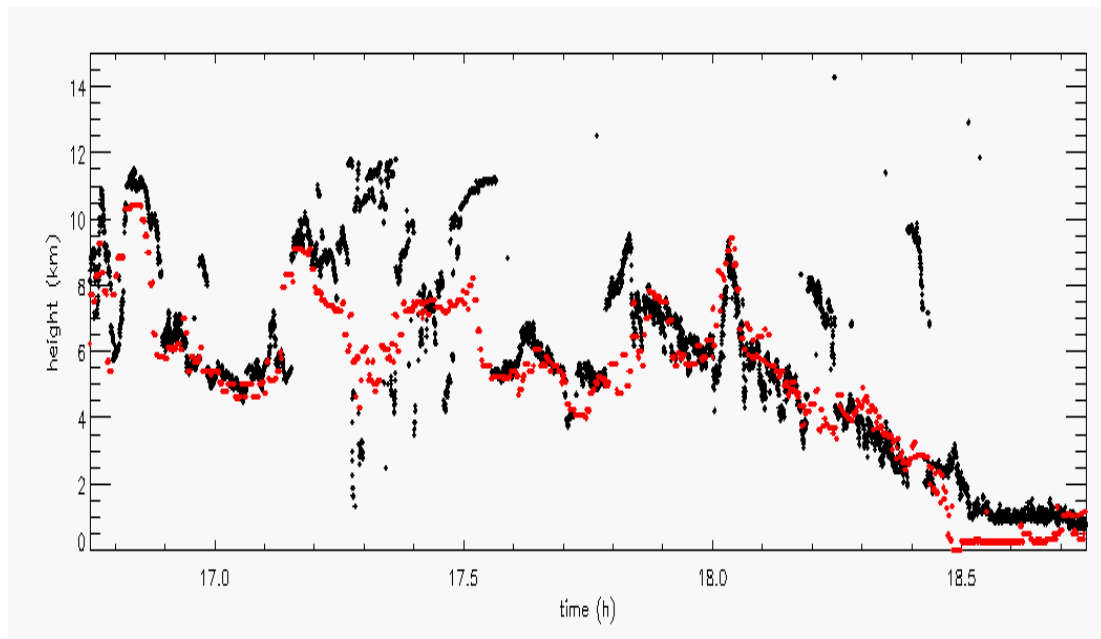


Figure 3: GOES-12 (red) and CPL (black) cloud heights for 5 December 2003 from 1700 to 1830 UTC.

3.2. Comparison of CO₂/IRW slicing and H₂O/IRW intercept heights

Comparison of these height assignment techniques was accomplished with data from the GOES-12 on 2-4 June 2004. Cloud elements were selected by the autowindco procedure (Merrill et al., 1991) that divides the entire image into cells (roughly 50 km on a side) and selects targets based on the overall brightness and contrast of the scene. Height assignments were made with all three methods described above. Mean cloud top pressures for all the height assignments using a single technique are calculated and the root mean square (rms) scatter about that mean is also calculated; the scatter is due to natural variability in the cloud heights as well as technique inaccuracy. The rms deviation of heights for all the tracers using one technique with respect to those using another technique are also presented; this value represents the deviation of one technique with respect to the other.

Clouds were separated into water or ice classes using coincident MODIS 8.5 and 11 μm measurements; Figure 4a presents MODIS cloud thermodynamic phase determinations for 422 UTC 3 June 2004. Figure 4b shows the associated GOES-12 Cloud Top Pressure Derived Product Image using the CO₂/IRW slicing technique and IRW technique to infer cloud top pressure.

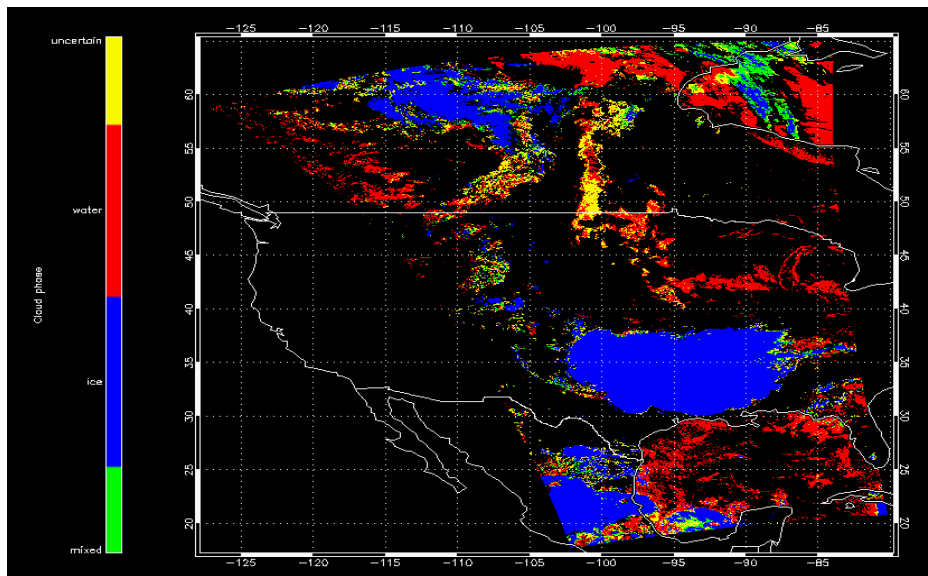


Figure 4a: MODIS IR cloud phase with ice clouds (blue), water clouds (red), mixed phase clouds (green), and uncertain phase (yellow) for 0422UTC 3 June 2004.

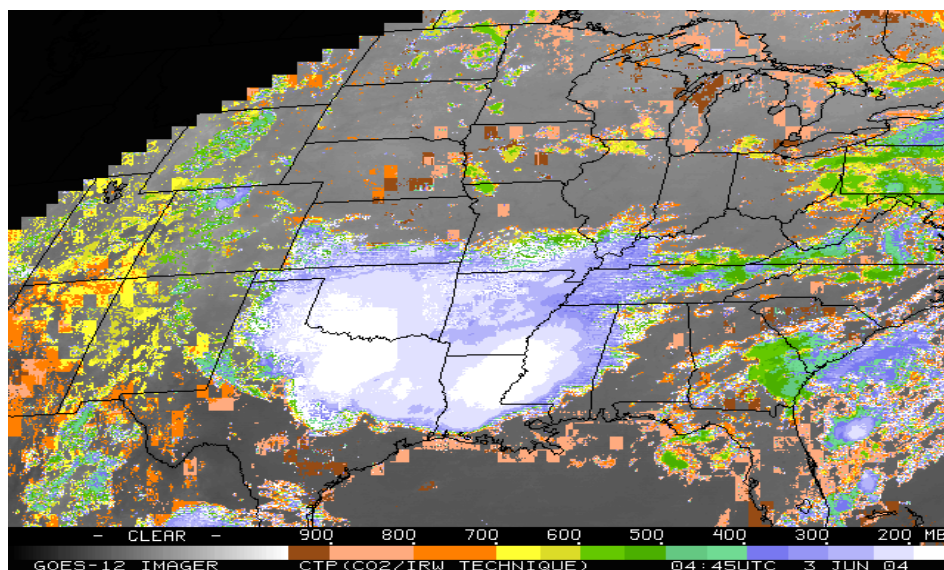


Figure 4b: Corresponding GOES-12 CO₂/IRW Slicing Cloud Top Pressure Derived Product Image.

Ice clouds

Table 1: IRW, CO₂/IRW, and H₂O/IRW height assignments for ice cloud tracers using GOES-12 radiances from 2-4 June 2004.

(655 tracers)	Mean CTP	RMS wrt Mean	RMS Deviation wrt CO ₂ /IRW	H ₂ O/IRW
IRW	476	126	146	139
CO ₂ /IRW	271	98	--	109
H ₂ O/IRW	247	85	109	--

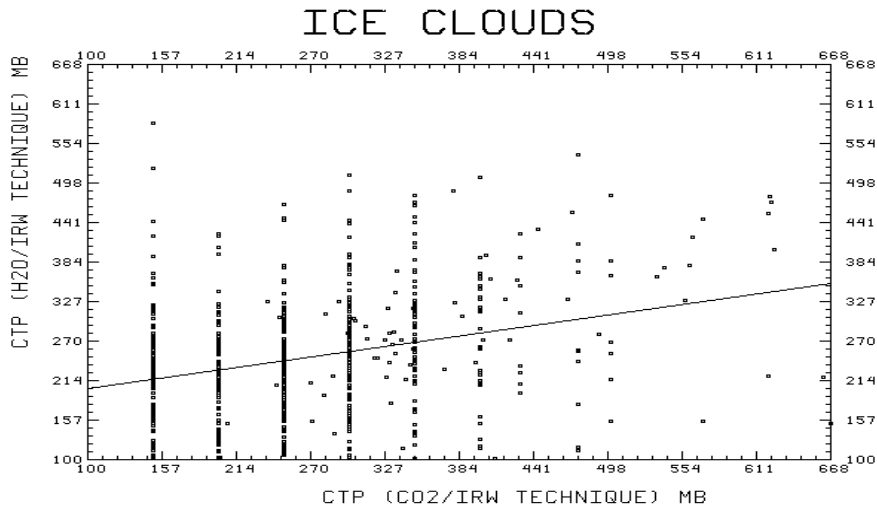


Figure 5: H₂O intercept (y-axis) compared with CO₂ slicing cloud height assignments in ice clouds for 2-4 June 2004.

The H₂O/IRW height assignments in these ice clouds are on the average 25 hPa higher in the atmosphere than the CO₂/IRW height assignments. The IRW heights, without benefit of any semi-transparency correction, are about 200 hPa lower in the atmosphere than the CO₂/IRW height assignment on the average. Figure 5 shows the scatter plot of H₂O/IRW and CO₂/IRW cloud top pressures; H₂O/IRW and CO₂/IRW estimates show large disagreement at all levels. For all of the cloud tracers selected for vector calculation in the scenes on 2-4 June 2004, the CO₂/IRW slicing algorithm produce a height for all of the tracers and the H₂O/IRW intercept failed for about 50% of the tracers. This is in part due to the instability of the H₂O/IRW cluster extrapolation to cloud top pressure. The CO₂/IRW technique is more robust and provides a CTP assignment more often in ice clouds.

When the two techniques are compared as a function of the effective cloud amount (see Figure 6). For thin ice clouds, the H₂O/IRW intercept heights are lower than the CO₂/IRW slicing heights (as the weighting functions in Figure 2 indicate). For thick ice clouds, the H₂O/IRW intercept heights are slightly higher than the CO₂/IRW slicing heights. The difference and variance between the two techniques decreases with increasing cloud amount.

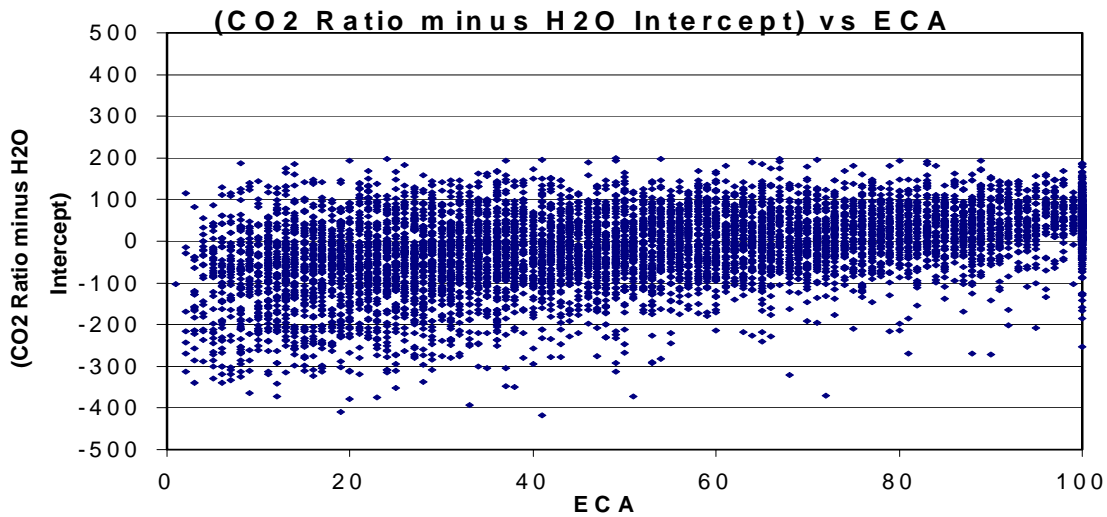


Figure 6: Difference of cloud top pressures estimated by CO₂/IRW slicing minus H₂O/IRW intercept as a function of effective cloud amount (estimated from CO₂/IRW slicing technique).

Water Clouds

Table 2: IRW, CO₂/IRW, and H₂O/IRW height assignments for water cloud tracers using GOES-12 radiances from 2-4 June 2004.

(38 tracers)	Mean CTP	RMS wrt Mean	RMS Deviation wrt CO ₂ /IRW	RMS Deviation wrt H ₂ O/IRW
IRW	710	99	185	198
CO ₂ /IRW	535	153	--	169
H ₂ O/IRW	431	82	169	--

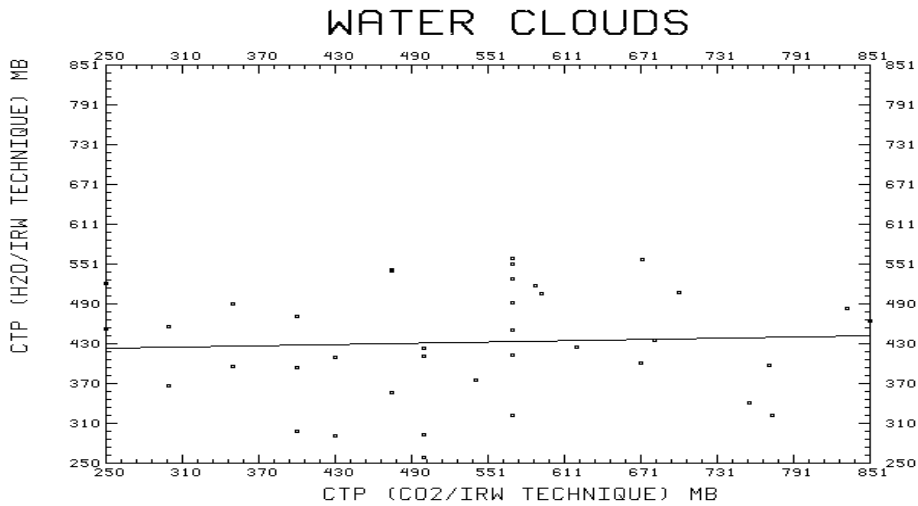


Figure 7: H₂O intercept (y-axis) compared with CO₂ slicing cloud height assignments in water clouds for 2-4 June 2004.

The H₂O/IRW height assignments in these water clouds are on the average 100 hPa higher in the atmosphere than the CO₂/IRW height assignments. The IRW are about 175 hPa lower in the atmosphere than the CO₂/IRW height assignment on the average. Figure 7 shows the scatter plot of H₂O/IRW and CO₂/IRW cloud top pressures; the H₂O/IRW show little scatter about a mean height while CO₂/IRW shows a larger range of possibilities. Neither technique is well suited for these cloud height determinations; (a) the

H₂O channel weighting function peaks too high in the troposphere to show much sensitivity to these water clouds and (b) the CO₂ and IRW channel cloud emissivities are no longer similar in water clouds so that the ratio approach fails to generate a reliable solution for the cloud top pressure. For all of the cloud tracers selected for vector calculation in the scenes on 2-4 June 2004, the CO₂/IRW slicing algorithm produce a height for all of the tracers and the H₂O/IRW intercept failed for about 85% of the tracers.

4. CONCLUSIONS

GOES-12 results presented in this paper suggest that the CO₂/IRW slicing technique produces cloud heights in good agreement with lidar determinations; occasional thin cloud eludes the CO₂/IRW slicing technique and the backup IRW technique then places these thin clouds roughly 5 km too low in the troposphere. H₂O/IRW intercept and the CO₂/IRW slicing techniques for inferring the heights of semi-transparent ice cloud elements produce similar results on average, but individual cloud height comparisons differ considerably. The CO₂/IRW slicing technique is more robust (has fewer failures in producing cloud top pressure for a set of cloud tracers). The IRW technique consistently places the semi-transparent cloud elements too low in the atmosphere by roughly 200 hPa; only in more opaque clouds does it perform adequately.

The CO₂/IRW slicing technique seems to produce the best cloud heights of the three approaches for high thin ice clouds. These results are similar to those presented at the last International Winds Workshop in May 2002.

5. REFERENCES

Baum, BA, Soulen, PF, Strabala, KI, King, MD, Ackerman, SA, Menzel, WP, Yang, P (2000) Remote sensing of cloud properties using MODIS Airborne Simulator imagery during SUCCESS. II. Cloud thermodynamic phase. *J. Geophys. Res.*, **105**, 11781-11792

Bennartz, R., and J. Fischer, 2000: A modified *k*-distribution approach applied to narrow band water vapor and oxygen absorption estimates in the near infrared. *J. Quant. Spectrosc. Radiat. Transfer*, **66**, 539–553.

Clough, S. A., M. J. Iacono, and J.-L. Moncet, 1992: Line-by-line calculation of atmospheric fluxes and cooling rates: Application to water vapor. *J. Geophys. Res.*, **97**, 15 761–15 785.

Kratz, D. P., 1995: The correlated *k*-distribution technique as applied to the AVHRR channels. *J. Quant. Spectrosc. Radiat. Transfer*, **53**, 501–517.

Menzel, W. P., W. L. Smith, and T. R. Stewart, 1983: Improved cloud motion wind vector and altitude assignment using VAS. *J. Clim. Appl. Meteor.*, **22**, 377-384.

Merrill, R. T., W. P. Menzel, W. Baker, J. Lynch, and E. Legg, 1991: A report on the recent demonstration of NOAA's upgraded capability to derive cloud motion satellite winds. *Bull. Amer. Meteor. Soc.*, **72**, 372-376.

Nieman, S. J., J. Schmetz and W. P. Menzel, 1993: A comparison of several techniques to assign heights to cloud tracers. *J. Appl. Meteor.*, **32**, 1559-1568.

Nieman, S. J., W. P. Menzel, C. M. Hayden, D. Gray, S. T. Wanzong, C. S. Velden, and J. Daniels, 1997: Fully automated cloud drift winds in NESDIS operations. *Bull. Amer. Meteor. Soc.*, **78**, 1121-1133.

Schmetz, J., K. Holmlund, J. Hoffman, B. Strauss, B. Mason, V. Gaertner, A. Koch, and L. van de Berg, 1993: Operational cloud motion winds from METEOSAT infrared images. *J. Appl. Meteor.*, **32**, 1206-1225.

Stamnes, K., S.-C. Tsay, W. Wiscombe, and K. Jayaweera, 1988: A numerically stable algorithm for discrete-ordinate-method radiative transfer in multiple scattering and emitting layered media. *Appl. Opt.*, **27**, 2502–2509.

Szejwach, G., 1982: Determination of semi-transparent cirrus cloud temperatures from infrared radiances: application to Meteosat. *J. Appl. Meteor.*, **21**, 384.

Wiscombe, W. J., 1977: The delta-*M* method: Rapid yet accurate radiative flux calculations for strongly asymmetric phase functions. *J. Atmos. Sci.*, **34**, 1408–1422.